INTERNATIONAL JOURNAL ON INFORMATICS VISUALIZATION

journal homepage : www.joiv.org/index.php/joiv

Lightweight Generative Adversarial Network Fundus Image Synthesis

Nurhakimah Abd Aziz [a], Mohd Azman Hanif Sulaiman [a], Azlee Zabidi [b], Ihsan Mohd Yassin [c,*], Megat Syahirul Amin Megat Ali [c], Zairi Ismael Rizman [d]

[a] School of Electrical Engineering, College of Engineering, Universiti Teknologi MARA, Shah Alam, Selangor, Malaysia
[b] Faculty of Systems & Software Engineering, College of Computing & Applied Sciences, Universiti Malaysia Pahang, Pahang, Malaysia
[c] Microwave Research Institute, Universiti Teknologi MARA, Shah Alam, Selangor, Malaysia
[d] School of Electrical Engineering, College of Engineering, Universiti Teknologi MARA, Dungun, Terengganu, Malaysia
Corresponding author: *ihsan.yassin@gmail.com

***Abstract*—Blindness is a global health problem that affects billions of lives. Recent advancements in Artificial Intelligence (AI), (Deep Learning (DL)) has the intervention potential to address the blindness issue, particularly as an accurate and non-invasive technique for early detection and treatment of Diabetic Retinopathy (DR). DL-based techniques rely on extensive examples to be robust and accurate in capturing the features responsible for representing the data. However, the number of samples required is tremendous for the DL classifier to learn properly. This presents an issue in collecting and categorizing many samples. Therefore, in this paper, we present a lightweight Generative Neural Network (GAN) to synthesize fundus samples to train AI-based systems. The GAN was trained using samples collected from publicly available datasets. The GAN follows the structure of the recent Lightweight GAN (LGAN) architecture. The implementation and results of the LGAN training and image generation are described. Results indicate that the trained network was able to generate realistic high-resolution samples of normal and diseased fundus images accurately as the generated results managed to realistically represent key structures and their placements inside the generated samples, such as the optic disc, blood vessels, exudates, and others. Successful and unsuccessful generation samples were sorted manually, yielding 56.66% realistic results relative to the total generated samples. Rejected generated samples appear to be due to inconsistencies in shape, key structures, placements, and color.**

***Keywords*— Generative Adversarial Network (GAN); fundus; artificial intelligence; data synthesis.**

Manuscript received 21 Dec. 2021; revised 18 Feb. 2022; accepted 29 Mar. 2022. Date of publication 31 May 2022.

I. Introduction

Globally, there are an estimated 2.2 billion blind people, of which at least 1 billion have vision problems that could have been avoided or are still unresolved [1]. Among the major causes of blindness is Diabetic Retinopathy (DR), a complication of diabetes mellitus [2]. It can cause complete blindness if left untreated [3]. Therefore, early detection and intervention are paramount. DR is caused by hyperglycemia, which leads to blood vessel clots in the retina. Left untreated, the blockages cause vascular disorder, blurred vision, and blindness [3]. DR is of particular concern since it is estimated that more than 600 million individuals will have diabetes by 2040, with 200 million expected to have DR as a consequence of the condition [4]–[6]. Furthermore, DR is currently the leading cause of blindness in the global working-age population [2]. Early intervention (screening and treatment) can prevent blindness [7]. Fundus images provide an interesting non-invasive diagnostic opportunity as the retina's intricate structure provides a non-invasive wealth of information for ophthalmic diagnosis [8]–[13].

As a fundamental pillar of Industrial Revolution 4.0, DL has received tremendous attention in research, especially in medical image analysis [4]. Relative to conventional AI, DL has been proven to excel in many domains. DL models allow the construction of multi-layered computational models that represent the data with increased levels of abstraction [14]. DL has shown potential as a method for quick automated diagnosis [7], particularly in areas with a low ophthalmologist-to-patient ratio [15].

Many works have been done on AI computer-based disease diagnosis. They typically require much data to sufficiently understand the data distribution to adapt to previously unseen data variabilities robustly. In certain cases, the number of data required to train is insufficient or imbalanced, leading to issues with classifier robustness [14], [15]. Data augmentation (a set of techniques to enhance the quality and diversity of

datasets) can be used to mitigate this issue. Data augmentation techniques are particularly important for AI-based diagnostic systems [2].

Recent advancements in the field of Generative Adversarial Networks (GAN) have elevated them to a fascinating tool for creating realistic data [2], [16]. GANs are composed of two neural networks that compete with each another. The first network, dubbed the generator, learns to build images from the statistical distribution of training data. On the other hand, the discriminator learns to differentiate between real images and those made by the generator. The antagonistic interplay between the generator and discriminator gradually improves both networks until the generator produces impersonations of such high quality that the discriminator accepts them as originals [17], [18].

This paper proposes a GAN to synthesize normal and diseased fundus images. The structure of the GAN was based on the works of Liu et al. [19]. We introduce two datasets as training inputs for the GAN with no pre-processing to help preserve data variability. We demonstrate the effectiveness of the GAN by analyzing the outputs produced by the GAN post-training. The discoveries in this paper may be used to train robust AI-based classifiers. Additionally, the synthesized images can be used as a diagnostic teaching aid for students in medical schools. The rest of this paper is organized as follows: Section I-B presents the literature review, followed by the methodology in Section II. Results and discussions are presented in Section III. Finally, concluding remarks are presented in Section IV.

A. Applications of DL on Fundus Images

This section presents recent literature related to applications of DL on Fundus Images. DL appears to be primarily used for image quality enhancement (Section I-B-1), data synthesis (Section I-B-2), detection of structures in the fundus image (Section I-B-3), and diagnosis of disease severity (Section I-B-4). Each application is described in the following sections.

1) Image Quality Enhancement: Given the importance of fundus images for medical diagnosis, the quality of the image is paramount for accuracy, especially in automated computer-based applications [13], [20]. This section details some applications of AI (primarily GAN) in fundus image quality enhancement.

A modified version of the Pix2Pix GAN (Pix2Pix Fundus Oculi Quality Enhancer (P2P-FOQE)) was presented in [10] to enhance the quality of fundus images. The P2P-FOQE network removed artifacts and normalized the brightness and contrast to improve fundus image quality. To test the network, the authors collected a set of fundus images from Kaggle and classified them into three categories depending on the quality of the images – bad, usable, and good. The proposed network significantly improved the quality of the images across all categories by 29.49% to 72.33% while passing evaluations from specialist ophthalmologists.

A similar work by Cheng et al. [9] used Least-Squared GAN (LS-GAN) to enhance the quality of fundus images. Tested using Peaky Signal to Noise Ratio (PSNR) and Structural Similarity Index Measure (SSIM). Aims to preserve structural details (such as blood vessels) in the image and enhance any degradations present in the image. Comparing the proposed method and other established GAN structures demonstrates its effectiveness in enhancing the fundus images.

In Priya and Sathiaseelan [11], a Super Resolution GAN (SRGAN) U-Net structure enhanced fundus images for blood vessel recognition. The SRGAN intelligently supersizes the image by filling out absent features from the original low-resolution image. Managed to improve overall precision of blood vessel segmentation by 0.736%. Similarly, in Cheng et al. [13], GAN was used to enhance degraded fundus images. The GAN structure was modified to incorporate a contrastive loss function in the encoder (generator) network. Additionally, a priori loss function retains localized semantic information in the fundus image. The contrastive approach managed to obtain highly accurate enhancement while preserving local details.

CNNs have also been used to improve the quality of fundus images [3]. Bhatkalkar et al. [20] used CNN to automatically assess the quality of fundus images based on the optic disc's visibility. Transfer learning training was performed on the Inception v3 CNN architecture, and the authors obtained excellent classification accuracy on several publicly available databases.

Xu et al. [8] proposed a fundus and angiography image fusion method in Non-Subsampled Contourlet Transform (NSCT) to localize Central Serous Chorioretinopathy (CSCR). Original images were decomposed into high and low-frequency components. A pulse-coupled neural network was then used to fuse the components, adding important details to the original images. The method has been superior to the baseline Multi-Scale Transform (MST) method.

2) Data Synthesis: Mirabedini et al. [14] utilized GAN to synthesize fundus samples for training other types of classifiers. Data scientists face a common problem because DR classifiers are trained on imbalanced datasets (for example, there are different numbers of normal vs. diseased samples). This is because the diseased fundus images are relatively difficult to encounter compared to normal ones. Using the balanced dataset (combination of real and synthesized fundus images), the classification accuracy was 89%, a 7% improvement over the unbalanced dataset from Kaggle.

3) Detection of Important Structures in Fundus Images: Substantial works have also focused on detecting important structures in the fundus image, e.g., blood vessels, optic disc, exudates, etc. Rammy et al. [12] proposed a deep learning-based strategy for retinal vascular segmentation. The proposed Conditional Patch-based Generative Adversarial Network (CPGAN) purpose was to acquire improved discriminative features for thick and thin vessels in the fundus image. A loss term was combined with the primary objective function to learn low-frequency edges, and a patch-based discriminator was used to learn minor fluctuations and sharp edges of high-resolution blood vessels. The model demonstrated vastly efficient performance in segmenting thick and thin vascular pixels from non-vascular pixels by incorporating the additional loss function and patch-based discriminator.

In AlGhamdi [21], a CNN called RetinaNet was used to detect and segment optic disc in fundus images. The OD is important to detect neovascularization indicative of glaucoma. The network consists of one backbone network and two subnetworks. The backbone network was modeled after the established DenseNet architecture, while the two subnetworks were responsible for object recognition and localization of the OD. Tests on several publicly available datasets demonstrate the effectiveness of the proposed method. Optic disc detection and removal in fundus images is an important step for diagnosing glaucoma. As optic disc exhibits similar characteristics to glaucoma, they can be misinterpreted as a false positive in the detection of glaucoma. Realizing the importance, Liu et al. [22] suggested a GAN-based approach to localize and segment the optic disc. The GAN was trained to construct a probability map indicating the probability that the pixel is an optic disc. Experiments on the DRISHTI-GS dataset demonstrate the method's robustness in localizing the optic disc in normal, low contrast, and additional artifacts.

He et al. [23]automatically used CNN to localize hard exudates in a fundus image. The researchers opted for the Hue, Saturation, Value (HSV) color space to compensate for the low brightness and contrast in the images. The green channel from the color space was extracted for classification because of its highest contrastive properties. The CNN was then used to classify the pixels into either exudate or non-exudate. The proposed method obtained approximately 70% - 96% accuracy on the IDRiD dataset.

4) Diagnosis of DR Severity: CNN is typically used to grade the severity of DR based on the fundus image. Researchers working in this area repurpose an established CNN structure using transfer learning to retrain and repurpose classifier networks [24]. Transfer learning was used in Wang and Schaefer [15], [24] to repurpose a CNN to discriminate between normal and neovascularized fundus images. Several established CNN network structures were examined: the AlexNet, GoogleNet, VGG16, and others. In Wang and Schaefer [15], the authors used transfer learning to repurpose the MobileNet v2 network to assess the severity of DR on an imbalanced dataset.

Wang et al. [25] used the DeepMT-DR CNN to grade low-quality fundus images. The DeepMT-DR combines the task of Image Super-Resolution (ISR) (to boost details in the image) and grading the DR severity based on the ISR output. When tested on two publicly available datasets, the proposed method significantly outperforms other state-of-the-art methods.

II. Material And Method

A. Hardware and Software Specifications

The specifications of the hardware used in the experiments are shown in Table 1.

TABLE I
SPECIFICATIONS OF HARDWARE USED

Item	Specification
Central Processing Unit (CPU)	AMD Threadripper 3990x
Graphics Processing Unit (GPU)	4 × GTX 1080 Ti
Random Access Memory (RAM)	64 GB
Operating System	Linux Ubuntu 20.04.3 LTS

B. Flowchart of Experiments

The flowchart for the experiment is shown in Fig. 1. The experiment consists of four main steps, as described in Section II-B-1 to Section II-B-4.

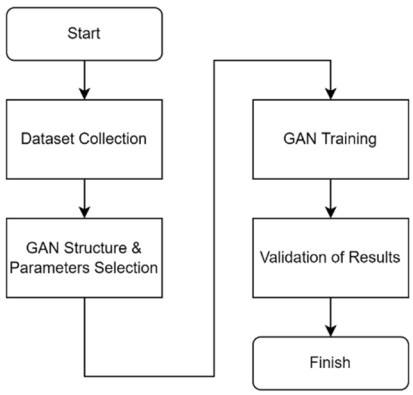

Fig. 1 Experiment flowchart

1) Data collection: The dataset used in the experiment were sourced from the Kaggle website:

Dataset 1 - Ocular Disease Recognition (ODIR) dataset by Larxel (https://www.kaggle.com/ andrewmvd/ ocular-disease-recognition-odir5k): This dataset consists of left and right fundus colour images of 5,000 patients diagnosed by medical professionals as suffering from eight medical conditions. It was collected from Shanggong Medical Technology Co., Ltd. The company has different medical facilities throughout China. The images were acquired using various devices (such as Canon, Zeiss and Kowa) resulting in various image resolutions and qualities. The images are categorized as Normal, Diabetes, Glaucoma, Cataract, Age-related Macular Degeneration, Hypertension, Pathological Myopia, and others. The ODIR dataset consists of 8,000 fundus images stored in the Joint Pictures Expert Group (JPEG) format.

Dataset 2 - Retinal Disease Classification (RDC) dataset by Larxel (https://www.kaggle.com/ andrewmvd/ retinal-disease-classification): The RDC dataset consists of 3,200 fundus images classified into 46 different diseases through consensus of two medical professionals. The RDC dataset are stored in the Portable Network Graphics format.

Both datasets were combined, producing the final 11,200 images. No pre-processing was applied to the images to preserve their variability and ensure the GAN's robustness to learn their features to synthesize new samples. Several samples from both datasets are shown in Fig. 2 and Fig. 3.

2) GAN structure and parameter selection: The GAN structure is based on the Lightweight GAN (LGAN) implementation [19], which is available at Liu et al. [26]. The network structure incorporates skip-layer excitation in the generator and self-supervised autoencoder layer in the discriminator. These adjustments significantly enhance the speed of high-resolution training with modest computational requirements [17], [18]. The reader is referred to Patil et al. [17] for information on the LGAN generator and discriminator architecture. The LGAN training parameters are listed in Table 2.

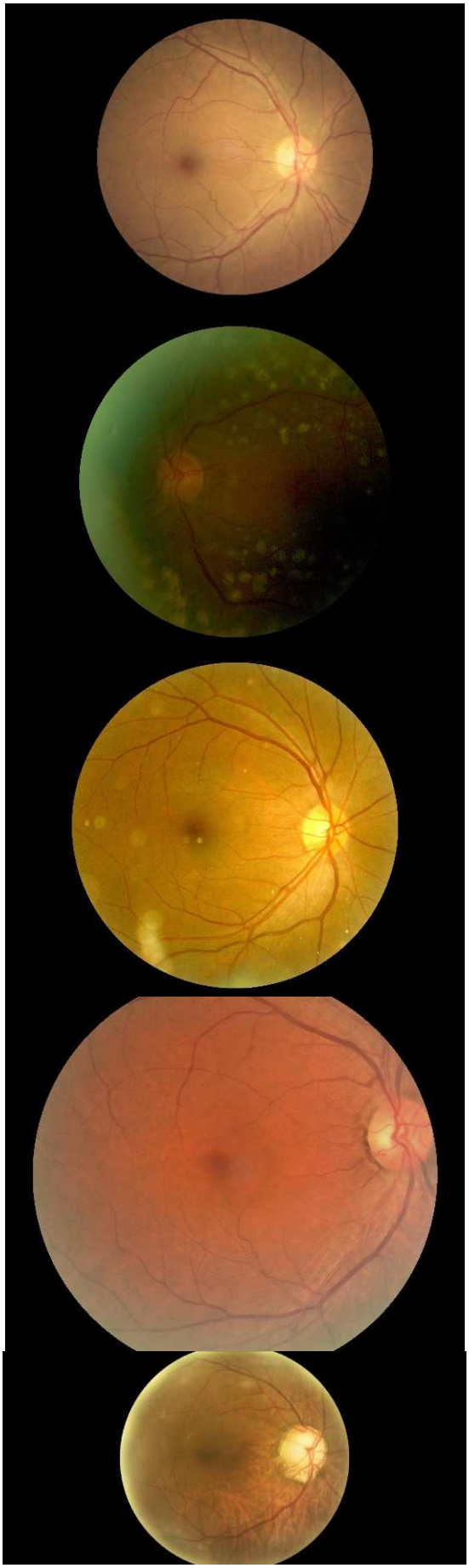

Fig. 2 Several samples from the ODIR dataset (Dataset 1)

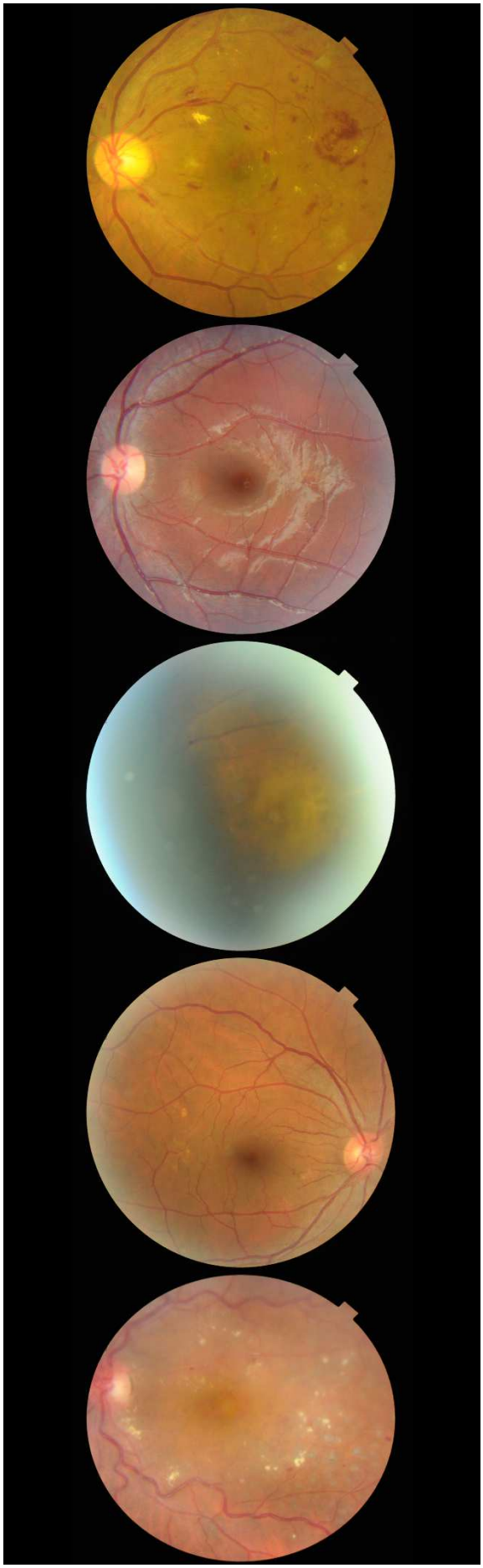

Fig. 3 Several samples from the RDC dataset (Dataset 2)

GAN training necessitates interaction and competition between two networks, the discriminator and the generator [27]. Both are simultaneously trained using the Adaptive Moment Estimation (ADAM) algorithm [28]. The ADAM algorithm was chosen due to its high computational efficiency (particularly for networks with many parameters) and low memory requirements [29]. Additionally, ADAM parameters require extremely less adjustment in comparison to standard backpropagation algorithms. The maximum number of epochs was set to 200,000. This value was found to be sufficient based on our preliminary experiments. Automatic Mixed Precision (AMP) is a technology by Nvidia [30]. It reduces the numerical precision of the weights to boost the computational speed while reducing the amount of GPU memory used with minimal effect on accuracy.

TABLE II
TRAINING PARAMETER VALUES

Parameter	Value
Training Algorithm	Adaptive Moment Estimation (ADAM)
Epochs	200,000
Automatic Mixed Precision (AMP)	Enabled
Output Size	1,024 × 1,024 pixels

3) GAN training: During training, an image preview was generated per 1,000 iterations. The preview was used to monitor the training progress of the LGAN.

4) Validation of results: The results were validated using two methods. The first method visually monitors the training performance of the network based on the quality of images generated to pre-emptively detect mode collapse. Mode collapse is a common problem in GAN training caused by the performance progress imbalance either from the generator or discriminator. Ideally, the generator and discriminator should gradually improve in tandem. However, if either the generator or discriminator improves drastically over the other, mode collapse will occur, affecting the quality of the synthesized images will be poor.

The second validation was performed post-training. This was done by synthesizing samples from the GAN and evaluating whether they were qualitatively realistic compared to the original data. The GAN-synthesized images were visually inspected for structural defects, e.g., no optic disc and unnaturally shaped structures in the fundus image. Fig. 4 shows common structures and anomalies in a fundus image. The presence and appearance of the structures and anomalies were examined closely when evaluating the synthesized LGAN samples.

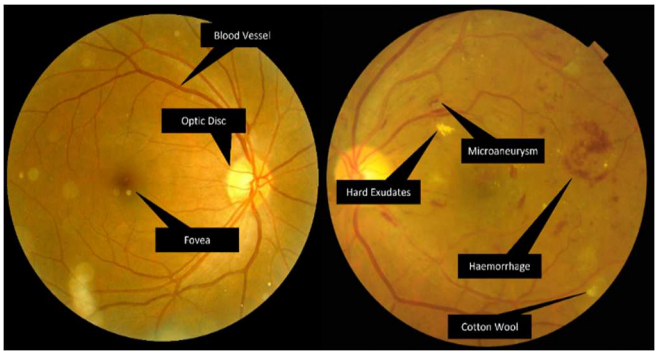

Fig. 4 Components in fundus images and DR anomaly structures [3]

III. Result And Discussion

Training time took approximately 67 hours. The training progression of the LGAN model is shown in Fig. 5 to Fig. 13. Initially, the samples appear to consist of irregular blobs on a black background. This observation is attributed to the unoptimized weights in the generator and discriminator. As training progressed, the structure and anomalies appeared to be more refined and consistently resembled the real training images, especially the position of the optic disc and blood vessels (Fig. 6 to Fig. 13). The color of the fundus also generally appears to be varied from yellow to shades of orange, red, and grey. These colors were also consistent with the training images. However, occasionally, there were irregularly formed shapes, as shown in the fourth sample in Fig. 9 and the seventh image in Fig. 10. There were also cases where the fundus colors were inconsistent, such as in the second and third images in Fig. 14.

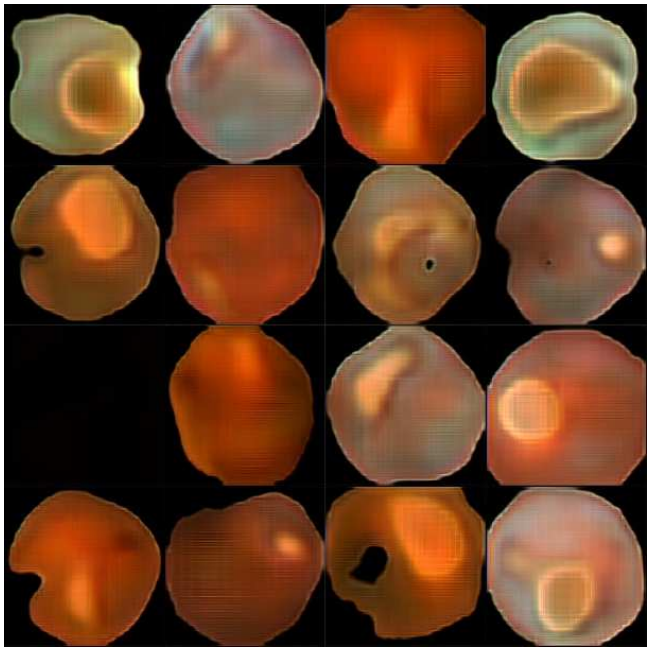
Fig. 5 Training progression (0 Epochs)

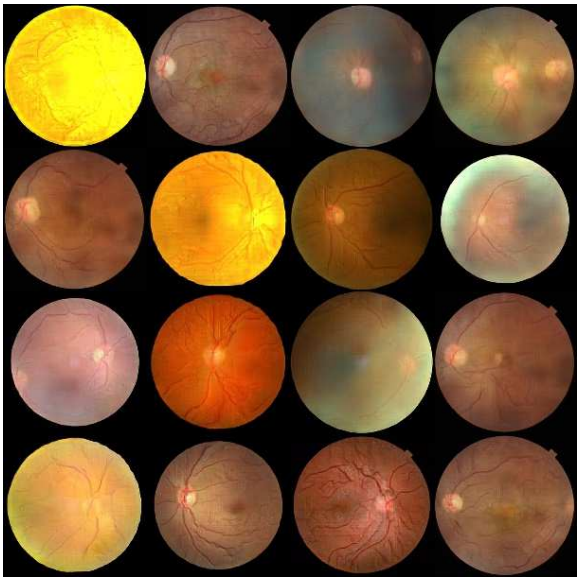
Fig. 6 Training progression (25,000 Epochs)

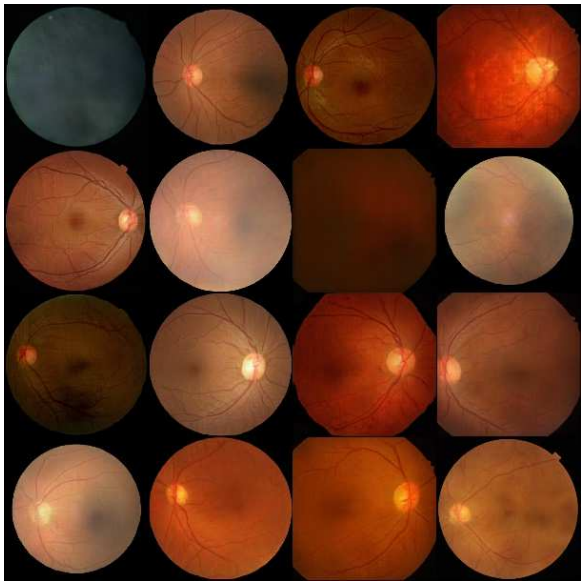

Fig. 7 Training progression (50,000 Epochs)

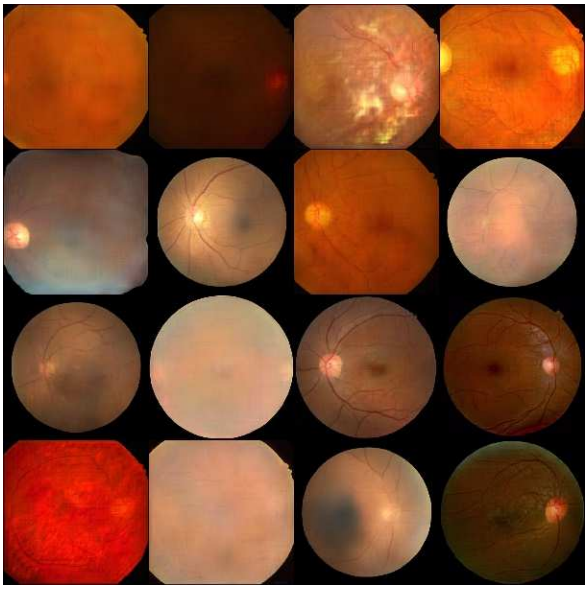

Fig. 8 Training progression (75,000 Epochs)

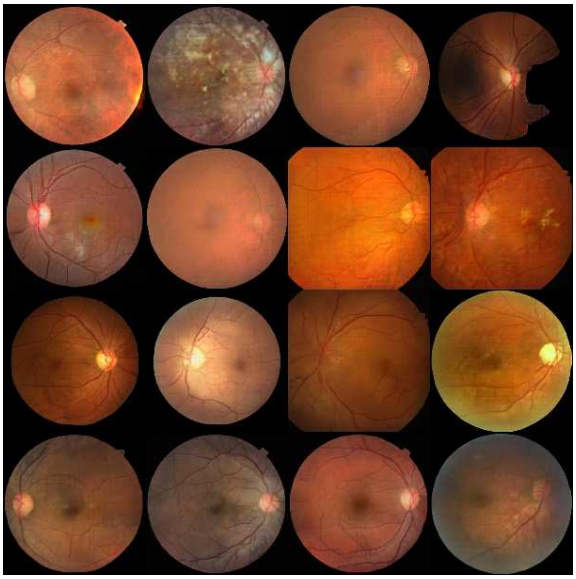

Fig. 9 Training progression (100,000 Epochs)

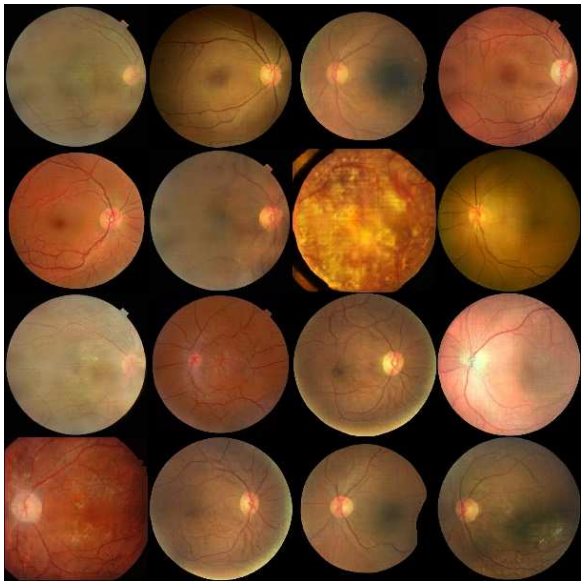

Fig. 10 Training progression (125,000 Epochs)

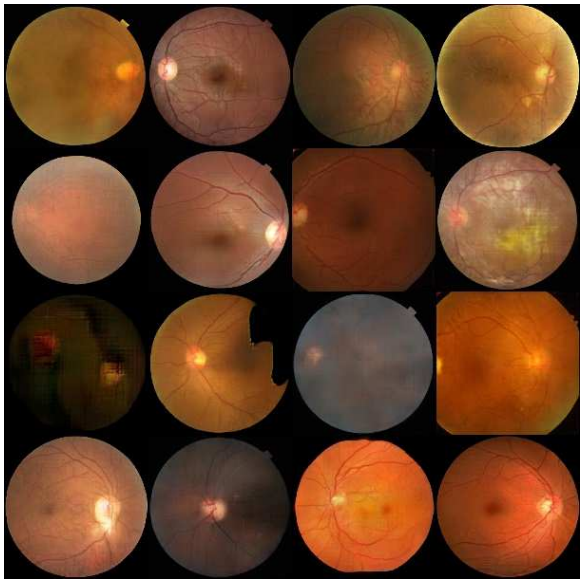

Fig. 11 Training progression (150,000 Epochs)

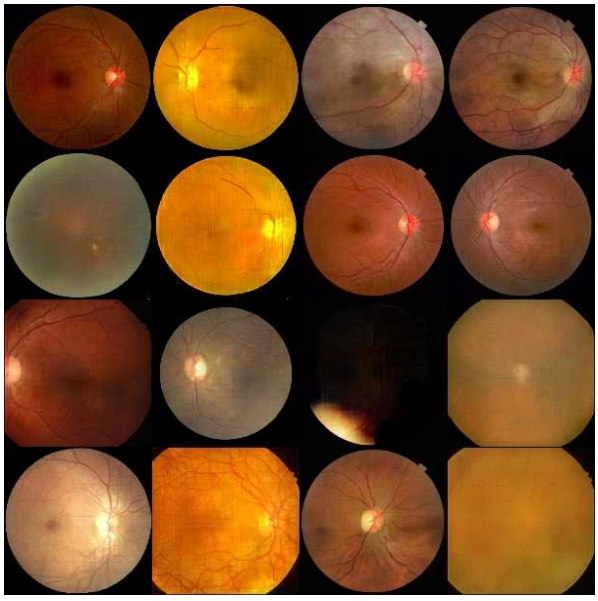

Fig. 12 Training progression (175,000 Epochs)

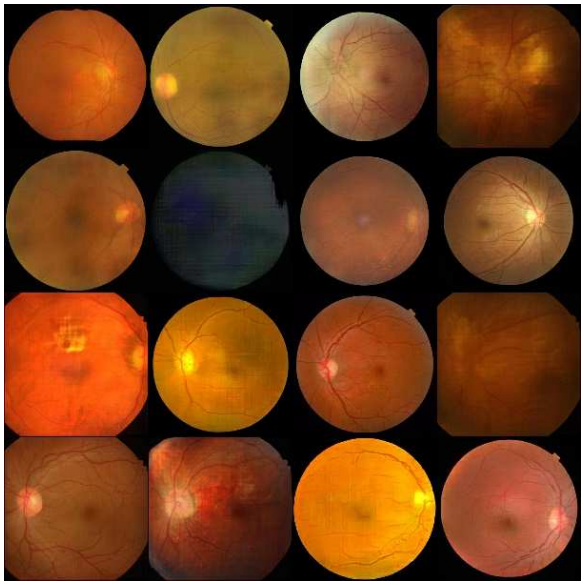

Fig. 13 Training progression (200,000 Epochs)

After training, the LGAN was then used to generate 1,210 fresh samples. These samples were examined based on color, structure, shape, anomalies, and appearance. Next, a decision was made whether to accept or reject the image depending on how realistic it appeared. The distribution of the images is shown in Table 3. Samples of accepted and rejected images are shown in Fig. 14 and Fig. 15. The generated results appear to skew towards normal types, and this is likely attributed to the number of samples used for training. As more normal samples were used for training data, the LGAN learned more features from them and generated more of those types of samples. The quality of the synthesized images appears acceptable at a resolution of 1,024 × 1,024 pixels, with fine details present and visible.

TABLE III
DISTRIBUTION OF 1,210 LGAN-SYNTHESIZED SAMPLES (POST-TRAINING)

Acceptable	685
Not Acceptable	525

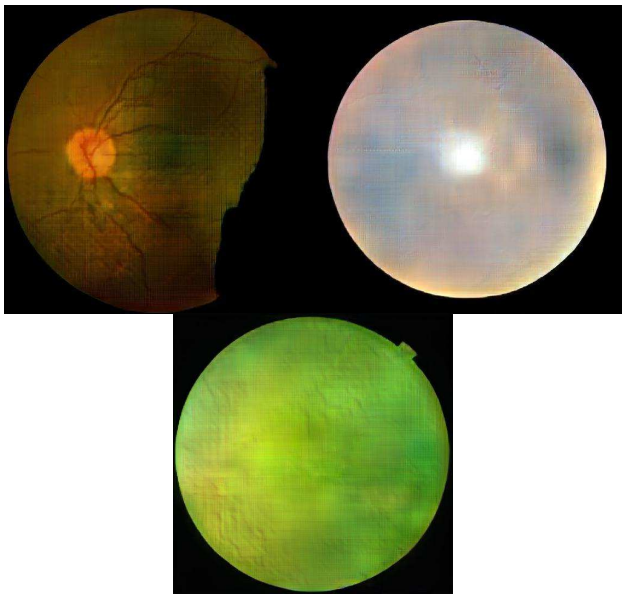

Fig. 14 Samples of rejected images due to shape, inconsistent features, and color

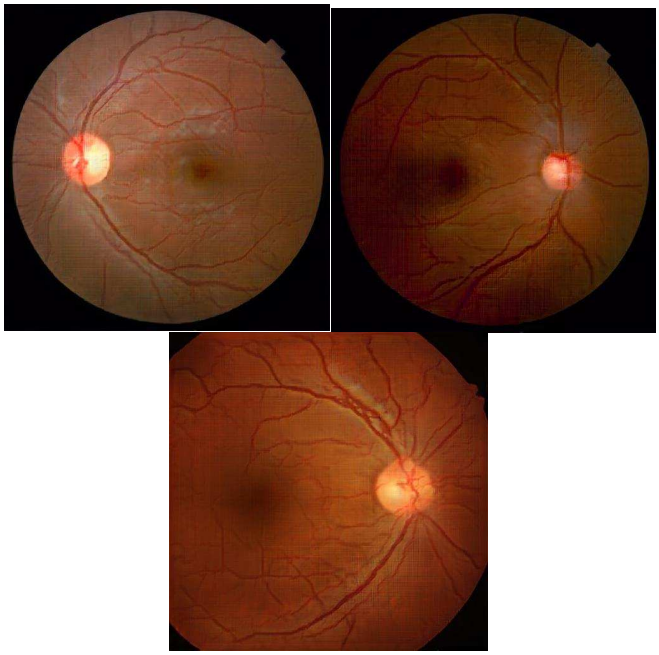

Fig. 15 Samples of accepted images (accurate placement of optic disc, visible blood vessels, consistent shape and color).

IV. CONCLUSION

A LGAN was repurposed to generate synthetic fundus images. The LGAN was trained on two publicly available datasets from Kaggle without any form of pre-processing. Experiments indicate that the generator and discriminator were able to generate realistic images by learning the distribution on the training images.

ACKNOWLEDGMENT

The authors gratefully acknowledge the Ministry of Higher Education, Malaysia for equipment support through the Long-term Research Grant Scheme (LRGS) 600-RMC/LRGS 5/3 (001/2020). Funds from Universiti Malaysia Pahang (Grant No: RDU200750) and infrastructure support from Universiti Teknologi MARA, Malaysia is gratefully acknowledged.

REFERENCES

[1] World Health Organization (WHO), "World Report on Vision," Geneva: WHO, 2019.

[2] Eisa Aghchehli and Malcolm Clarke, "Deep learning based data augmentation using Generative Adversarial Network in Diabetic Retinopathy: A Review," 2020, https://www.researchgate.net/profile/Eisa-Aghchehli-2/publication/339680691_deep_learning_based_data_augmentation_using_generative_adversarial_network_in_diabetic_retinopathy_a_review/links/5e6eaf47458515e5557fba74/deep-learning-based-data-augmentation-using-generative-adversarial-network-in-diabetic-retinopathy-a-review.pdf.

[3] N. Mukherjee and S. Sengupta, "In Search for the Optimal Preprocessing Technique for Deep Learning Based Diabetic Retinopathy Stage Classication from Fundus Images", doi: 10.21203/rs.3.rs-654484/v1.

[4] D. S. W. Ting *et al.*, "Artificial intelligence and deep learning in ophthalmology," *British Journal of Ophthalmology*, vol. 103, no. 2. BMJ Publishing Group, pp. 167–175, Feb. 01, 2019. doi: 10.1136/bjophthalmol-2018-313173.

[5] C.-I. Suciu, V.-I. Suciu, A. Cuţaş, and S. D. Nicoară, "Interleaved Optical Coherence Tomography: Clinical and Laboratory Biomarkers in Patients with Diabetic Macular Edema," *Journal of Personalized Medicine*, vol. 12, no. 5, p. 765, May 2022, doi: 10.3390/jpm12050765.

[6] C. Sabanayagam *et al.*, "Association of Diabetic Retinopathy and Diabetic Kidney Disease with All-Cause and Cardiovascular Mortality in a Multiethnic Asian Population," *JAMA Network Open*, vol. 2, no. 3, Mar. 2019, doi: 10.1001/jamanetworkopen.2019.1540.

[7] S. Mishra and S. Hanchate, "Detection of Diabetic Retinopathy from Fundus Images using Deep Learning:A Review." [Online]. Available: www.joics.net.

[8] J. Xu, C. Wan, W. Yang, B. Zheng, Z. Yan, and J. Shen, "A novel multi-modal fundus image fusion method for guiding the laser surgery of central serous chorioretinopathy," *Mathematical Biosciences and Engineering*, vol. 18, no. 4, pp. 4797–4816, 2021, doi: 10.3934/mbe.2021244.

[9] P. Cheng, L. Lin, Y. Huang, J. Lyu, and X. Tang, "I-SECRET: Importance-Guided Fundus Image Enhancement via Semi-supervised Contrastive Constraining," in *Lecture Notes in Computer Science (including subseries Lecture Notes in Artificial Intelligence and Lecture Notes in Bioinformatics)*, 2021, vol. 12908 LNCS, pp. 87–96. doi: 10.1007/978-3-030-87237-3_9.

[10] A. D. Pérez, O. Perdomo, H. Rios, F. Rodríguez, and F. A. González, "A Conditional Generative Adversarial Network-Based Method for Eye Fundus Image Quality Enhancement," in *Lecture Notes in Computer Science (including subseries Lecture Notes in Artificial Intelligence and Lecture Notes in Bioinformatics)*, 2020, vol. 12069 LNCS, pp. 185–194. doi: 10.1007/978-3-030-63419-3_19.

[11] S. Sathiya Priya and J. G. R. Sathiaseelan, "Enhanced Retina Blood Vessel Segmentation by Super Resolution Generative Adversarial Networks based U-Net," *Article in Indian Journal of Science and Technology*, vol. 14, no. 43, pp. 3246–3253, 2021, doi: 10.17485/IJST/v14i43.1502.

[12] S. A. Rammy, W. Abbas, N. U. Hassan, A. Raza, and W. Zhang, "CPGAN: Conditional patch-based generative adversarial network for retinal vessel segmentation," *IET Image Processing*, vol. 14, no. 6, pp. 1081–1090, May 2020, doi: 10.1049/iet-ipr.2019.1007.

[13] P. Cheng, L. Lin, Y. Huang, J. Lyu, and X. Tang, "Prior guided fundus image quality enhancement via contrastive learning," in *Proceedings - International Symposium on Biomedical Imaging*, Apr. 2021, vol. 2021-April, pp. 521–525. doi: 10.1109/ISBI48211.2021.9434005.

[14] S. Mirabedini, M. Kangavari, and J. Mohammadzadeh, "Diabetic retinopathy classification via Generative Adversarial Networks", [Online]. Available: www.isisn.org.

[15] L. Wang and A. Schaefer, "Diagnosing diabetic retinopathy from images of the eye fundus." [Online]. Available: https://machinethink.net/blog/mobilenet-v2/.

[16] F. Lateef, M. Kas, and Y. Ruichek, "Saliency Heat-Map as Visual Attention for Autonomous Driving Using Generative Adversarial Network (GAN)," *IEEE Transactions on Intelligent Transportation Systems*, pp. 1–14, 2021, doi: 10.1109/TITS.2021.3053178.

[17] S. O. Patil, V. v. Sajith Variyar, and K. P. Soman, "Speed Bump Segmentation an Application of Conditional Generative Adversarial Network for Self-driving Vehicles," *Proceedings of the 4th International Conference on Computing Methodologies and Communication, ICCMC 2020*, no. Iccmc, pp. 935–939, 2020, doi: 10.1109/ICCMC48092.2020.ICCMC-000173.

[18] J. Spooner, V. Palade, M. Cheah, S. Kanarachos, and A. Daneshkhah, "Generation of pedestrian crossing scenarios using ped-cross generative adversarial network," *Applied Sciences (Switzerland)*, vol. 11, no. 2, pp. 1–21, 2021, doi: 10.3390/app11020471.

[19] B. Liu, Y. Zhu, K. Song, and A. Elgammal, "Towards Faster and Stabilized GAN Training for High-Fidelity Few Shot Image Synthesis," in *Proc.of 2021 Int. Conf. on Learning Representations (ICLR2021)*, 2021, pp. 1–13. [Online]. Available: https://github.com/odegeasslbc/FastGAN-pytorch.

[20] B. Bhatkalkar, A. Joshi, S. Prabhu, and S. Bhandary, "Automated fundus image quality assessment and segmentation of optic disc using convolutional neural networks," *International Journal of Electrical and Computer Engineering*, vol. 10, no. 1, pp. 816–827, 2020, doi: 10.11591/ijece.v10i1.pp816-827.

[21] M. AlGhamdi, "Optic Disc Segmentation in Fundus Images with Deep Learning Object Detector," *Journal of Computer Science*, vol. 16, no. 5, pp. 591–600, 2020, doi: 10.3844/JCSSP.2020.591.600.

[22] Y. Liu, D. Fu, Z. Huang, and H. Tong, "Optic disc segmentation in fundus images using adversarial training," *IET Image Processing*, vol. 13, no. 2, pp. 375–381, Feb. 2019, doi: 10.1049/iet-ipr.2018.5922.

[23] X. He, R. Luo, T. Shou, and H. Xiao, "Automatic Detection of Hard Exudates in Retinal Fundus Images," 2021. [Online]. Available: www.aaai.org.

[24] W. Setiawan, M. I. Utoyo, and R. Rulaningtyas, "Transfer learning with multiple pre-trained network for fundus classification," *Telkomnika (Telecommunication Computing Electronics and Control)*, vol. 18, no. 3, pp. 1382–1388, 2020, doi: 10.12928/TELKOMNIKA.v18i3.14868.

[25] X. Wang, M. Xu, J. Zhang, L. Jiang, and L. Li, "Deep Multi-Task Learning for Diabetic Retinopathy Grading in Fundus Images." [Online]. Available: www.aaai.org.

[26] Bingchen Liu, Yizhe Zhu, Kumpeng Song, and Ahmed Elgamal, "Github - Lightweight GAN, Available: https://github.com/lucidrains/lightweight-gan," *https://github.com/lucidrains/lightweight-gan*, 2021.

[27] D. M. Vo, D. M. Nguyen, T. P. Le, and S. W. Lee, "HI-GAN: A hierarchical generative adversarial network for blind denoising of real photographs," *Information Sciences*, vol. 570, pp. 225–240, Sep. 2021, doi: 10.1016/j.ins.2021.04.045.

[28] D. P. Kingma and J. Ba, "Adam: A Method for Stochastic Optimization," Dec. 2014, [Online]. Available: http://arxiv.org/abs/1412.6980.

[29] Á. Arcos-García, J. A. Álvarez-García, and L. M. Soria-Morillo, "Deep neural network for traffic sign recognition systems: An analysis of spatial transformers and stochastic optimisation methods," *Neural Networks*, vol. 99, pp. 158–165, Mar. 2018, doi: 10.1016/j.neunet.2018.01.005.

[30] Xuyang Guo *et al.*, "Exploration of Automatic Mixed-Precision Search for Deep Neural Networks," 2019.